International Conference on Applied Energy 2020
Dec. 1 - Dec. 10, 2020, Bangkok / Virtual
Paper ID: 138

Flow Induce Vibration Energy Harvesting of Circular Oscillator Under Square Wake

Vahid Tamimi [1], Jian Wu [1*]
1 School of Energy Science and Engineering, Harbin Institute of Technology, Harbin, PR China

ABSTRACT

Modification of the immediate flow field by means of an upstream circular body has been effective in the energy harvesting improvement of circular oscillators. In this empirical study, the influence of square wake on the harnessed power and efficiency of circular oscillators is investigated. The subject has not been addressed by other researchers. The results show that the square wake has Improving effects on the mechanical power of circular oscillators but deteriorates the hydroelastic efficiency. The overall energy harvesting performance of circular oscillators under nearby square wake is slightly higher than that in single configuration but is almost half of that under circular wake.

Keywords: flow induced vibration, energy harvesting, square wake, circular oscillator

1. INTRODUCTION

Electricity production from renewable energy resources has seen a great advancement in the last two decades. However, the major portion of the clean electricity in the world is still generated from the potential power of dammed rivers. Considering other sources of hydropower, namely the run-of-river or tidal power, the capacity for hydroelectric power generation is much greater than the present production [1]. Therefore lately, considerable efforts have been concentrated on Flow Induced Vibration (FIV) as one of the main approaches to extract energy from fluid kinetic power [2, 3].

FIV energy harvesting includes numerous fluid kinetic energy conversion technologies [4]. In one classification, the FIV electricity generators can be divided into (i) typical spinning windmills and water turbines and (ii) recently developing transverse FIV harvesters. Hydrokinetic energy harvesting based on vortex excited vibration of bodies has been widely studied by researches, owing to its high power energy production capability. Bernitsas and Raghvan [5] first proposed Vortex Induced Vibration Aquatic Clean Energy (VIVACE) to extract energy from the transverse oscillation of a bluff body. Since then, several studies have been performed to improve VIVACE to a high-power energy harvester [6]. These studies can be grouped into two main categories: i) enhancement of the electromechanical coupling [7, 8] and ii) improvement of the hydroelastic performance of the system.

Lee and Bernitsas [9], Ma, Sun, Nowakowski, Mauer, and Bernitsas [10] and Sun, Kim, Nowakowski, Mauer, and Bernitsas [11] attempted to improve the hydroelastic performance by modifying the mechanical parameters such as stiffness, mass, and damping. At a constant flow field, the next important parameter that influences the hydroelastic response of the system is the cross-sectional characteristic of the oscillator. Improvement of the hydroelastic performance by means of geometrical modification is a complex task and requires in-depth knowledge of various types of fluid elastic instabilities and influencing parameters.

Geometrical modification through Passive Turbulence Control (PTC) was done by Chang, Kumar, and Bernitsas [12] and Park, Bernitsas, and Kumar [13] to remove VIV limitations and to increase the response of the system. Selectively located roughness strips were attached to the circular oscillators to enhance their hydroelastic performance. Barrero-Gil, Alonso, and Sanz-Andres [14], Abdelkefi, Hajj, and Nayfeh [15], Ding, Zhang, Wu, Maoa, and Jiang [16], Zhang, Xu, Liu, Lian, and Yan [17], Hemon, Amandolese, and Andrianne [18], and Tamimi, Naeeni, Zeinoddini, Seif, and Dolatshahi [19] studied the FIV energy harvesting potential of different rectangular, square, trapezoid, triangular and D-shape cross-sections. Much recently, Tamimi, Armin,

Selection and peer-review under responsibility of the scientific committee of the 12th Int. Conf. on Applied Energy (ICAE2020).

Shahvaghar-Asl, Naeeni, and Zeinoddini [20] reported a distinct higher energy harvesting performance of a galloping oscillator with right-angle isosceles triangular section against circular, square and diamond harvesters.

Along with mechanical system properties and geometrical characteristics of the oscillator, the other influencing parameter on the hydroelastic performance of the energy harvester is the approaching flow field. The immediate flow around the oscillator can primarily be modified by means of a similar upstream body. For two identical circular cylinders in a tandem arrangement, a sustained increase in the downstream cylinder excitation amplitude was noticed by Assi, Bearman, Carmo, Meneghini, Shervin, and Willden [21] and was called Wake Induced Vibration (WIV). They showed that at the similar wake, the downstream cylinder oscillates with the frequency of the wake stiffness. To benefit from this similar wake interference, Kim and Bernitsas [22] and Sun, Ma, Kim, Nowakowski, Mauer, and Bernitsas [23] used multiple-cylinder synergy to harness more energy per cylinder than a single circular cylinder.

With dissimilar upstream cylinder, the vortices arriving at the downstream oscillator have different Strouhal frequency than its vortices shed. Tamimi, Naeeni, Zeinoddini, and Bakhtiari [24] showed that the combination of these two frequencies improves the cross-flow responses and extends the lock-in range of the circular oscillator. Furthermore, the downstream cylinder oscillations occurred mainly at the upstream square cylinder Strouhal frequency. As will be examined later; the prevailing frequency of the upstream sharp edge square and its positive impacts on the response of the circular oscillator can make square wakes an effective method to improve the performance of FIV energy harvesters. To the best of authors' knowledge, the employment of square wakes as an approach to enhance the hydrokinetic energy harvesting performance of circular oscillators has not yet been explored. To fill this gap, present study investigates the influence of the square interfering bodies on the mechanical power and hydroelastic efficiency of a circular cylinder.

2. FIV ENERGY HARVESTER POWER AND EFFICIENCY

An FIV energy harvesting device is composed of two main parts: i) the mechanical and ii) the electromechanical subsystems. These two subsystems are shown in Fig. 1. In this paper the energy performance of the mechanical subsystem is investigated. The effects of the electromagnetic coupling on the energy harvesting performance of the system will be examined later in a completing study. The dynamic equation of motion for a single degree of freedom linear oscillator is presented in Eq. (1). In this equation M, C and K are the mechanical system mass, damping and stiffness, respectively. $y(t)$ denotes the displacement of the oscillator and dot means its derivative to the time. F_y is the fluid force acting on the unit length of the cylinder (L) in the crossflow direction and is defined by Eq. (2).

$$M\ddot{y} + C\dot{y} + Ky = F_y \qquad 1$$

$$F_y = \frac{1}{2}\rho U^2 D C_{fluid} \qquad 2$$

In Eq. (2) ρ is the fluid density, U is flow velocity, D is the characteristic length of the body and C_{fluid} is the instantaneous fluid lift force coefficient on the oscillator. Assuming the harmonic motion of the oscillator with the frequency of f and amplitude of Y, the mechanical power in one period of vibration (T) is simplified to Eq. (3).

$$P_{Me} = \frac{\int_0^T C\,\dot{y}^2 dt}{T} \qquad 3$$

The fluid power (P_w) is assumed as the kinetic energy of the flow over the area swept by the cylinder. Thus the hydroelastic efficiency (η_{He}) of the present oscillator can be calculated from Eq. (4).

$$\eta_{He} = \frac{P_{Me}}{P_w} = \frac{2 \times \int_0^T C\,\dot{y}^2 dt}{\rho U^3 (D + 2Y) L T} \qquad 4$$

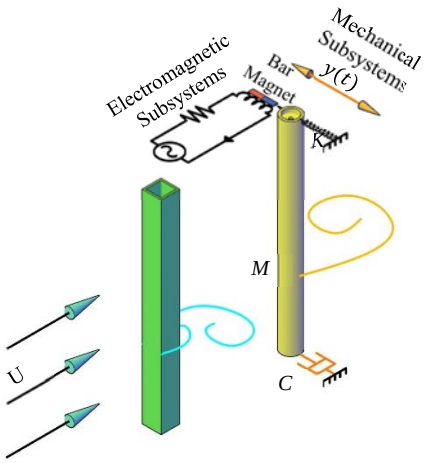

Figure 1. FIV energy harvester electromagnetic and mechanical subsystems.

3. EXPERIMENTAL SETUP

The experiments are performed in the towing tank of the Marine Engineering Laboratory at Sharif University of Technology (SUT), Iran. The test model is a Single Degree of Freedom (SDoF) circular cylinder with a diameter of 50 mm. The cylinder is tested in isolated and tandem arrangements. With the tandem configurations, the upstream cylinder is always fixed and has square cross-section (Fig. 1). Three center-to-center distances (S) are

investigated in this study: 200, 400 and 550 mm. The cylinder models are hollow with the submerged length of 500mm. A circular endplate with 260mm diameter is connected under each test cylinder to minimize the end effects on the cylinder responses. All test models and endplates are made of acrylic material.

The models are supported with an elastic SDoF device rigidly mounted under the moving carriage. The device comprises a pair of vertical spring-steel blade flexors bolted in parallel to two horizontal acrylic sheets. The cylinders are vertically installed to the lower horizontal slab through a force transducer. For the upstream cylinder, the cross-flow freedom of the elastic support is fixed employing two vertical acrylic slabs. These slabs connect the moving cap plate to the upmost plate attached to the carriage. Different parts of the elastic support are shown in the schematic view in Fig. 2. Recorded parameters include the transverse excitation and lift forces of the circular oscillator. Transverse displacements are measured by means of four strain gauges connected to the spring blades in a Wheatstone bridge configuration. The lift forces are recorded employing a shear-beam load cell. More details about the towing tank and experimental setup are provided in Zeinoddini, Tamimi, and Bakhtiari [25] and Tamimi, Naeeni, and Zeinoddini [26].

Table 1 presents the structural properties of the mechanical subsystem. The parameters include the total (M) and structural mass (m_s), structural damping coefficient (ζ) and natural frequencies (f_N) of the oscillating circular model. The system's damping and natural frequencies are estimated from free decay tests at still water. As will be seen later, because of the very low damping ratio of the current mechanical system, the efficiency of the FIV converter is considerably lower than that reported by other researchers. This fact, however, does not affect the accuracy and validity of the comparisons made between different configurations. By employing a system with optimum overall damping, efficiencies as high as 89% are achieved [22]. The Reynolds number in current studies ranges from 1.5×10^3 to 3.7×10^4 and the flow velocities (carriage speed) are approximately in the range of 0.04 to 0.85 m/s.

4. RESULTS AND DISCUSSIONS

4.1 Circular Oscillator under square wake

It is well-known that the frequency of vortices separating from a fixed body is defined by the Strouhal equation and depends on the flow Reynolds number (flow velocity and characteristic length of the body) and the body geometry (Strouhal number). For two identical circular bodies, the upstream wake frequency is similar to the downstream cylinder shedding outside the lock-in region. For the lock-in range and beyond, the downstream body shedding and vibrations get close to the system's natural and wake frequencies, respectively [21].

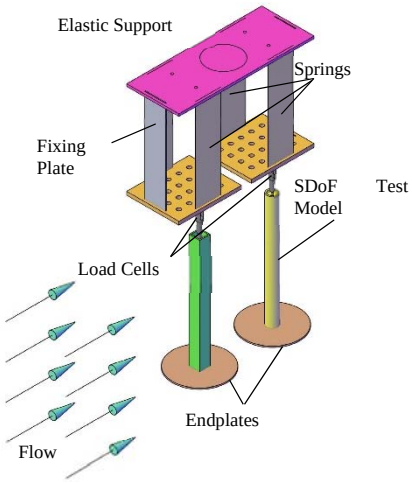

Figure 2. Schematic view of the experimental setup showing the elastic support, load cells, test models and endplates.

Table 1. Mechanical properties of the circular oscillator.

Stiffness	Total Mass	Structural Mass	Natural Frequency	Damping Coefficient
K (N/m2)	M (Kg)	m_s (Kg)	In water f_N (Hz)	In water ζ (%)
102	4.98	2.37	0.72	3.18

With the square sharp edge body at the upstream of the circular oscillator, Tamimi, Naeeni, Zeinoddini, and Bakhtiari [24] demonstrated that the oscillations mainly occur at the upstream body Strouhal frequency. The peak in the response amplitude reportedly occurred when the phase angle between the lift force and the displacement changed. These mark the reduced velocities of V_r=11 and 12 for the square upstream body in Fig. 3(a). The responses in Fig. 3(a) also show a smaller peak at the reduced velocities around 8 which can be referred to as the influence of the vortices shed from the downstream circular body. Furthermore, the figures depict that with the increase in the spacing ratio, the transverse responses generally reduce. The upstream square wake at close spacing increases the peak response of the circular oscillator by 37%.

The improving effects of the square wake on the mechanical power is much greater than the response amplitude (Fig. 3(b)). At S/D=4, the square cylinders' wake increases the harvested mechanical power of the isolated circular cylinder around 208%. The maximum

obtained mechanical power is around 0.123 W/m. At larger spacings, the square wake shows improving effects on the maximum harvested mechanical power by around 82% at S/D=8 and 24% at S/D=11. In general, the averaged harnessed power of the circular oscillator is reasonably improved by the upstream square wake.

Comparing to the isolated cylinder, the hydroelastic efficiencies are dissatisfying (Fig. 3(c)). This is mostly because, with square wakes the peaks of the response amplitudes are shifted to higher flow velocities with much greater power. The maximum hydroelastic transfer ratio is 2.21% for the upstream square wakes which is 69% lower than that of isolated cylinder. In spite of the lower maximum efficiency, the sharp peak efficiency of the single cylinder is widened by the upstream square wake.

4.2 Energy performance comparison

In this section the overall energy performance of a circular oscillator under square wake is compared with that in isolated configuration and under circular wake. Scoring the energy performance of the circular oscillator in different configurations is done by Technique for Order of Preference by Similarity to Ideal Solution (TOPSIS) method [27]. The averaged and maximum values of the hydroelastic efficiency and the mechanical power are selected as criteria of the TOPSIS algorithm. Considering that the averaged values imply a more general condition for each criterion, the weight value of the averaged and maximum power and efficiency are chosen equal to 0.3 and 0.2, respectively.

After creation of the decision matrix, the scores are normalized to create the dimensionless matrix. With the known diagonal weight matrix, the weighted normalized decision matrix (Table 2) is calculated. Using this decision matrix, the geometrical distance between each matrix element and the best and the worst solutions are calculated. Utilizing the computed geometrical distance matrix, the relative closeness of each alternative to the best condition can be calculated.

Table 2 gives the closeness of each alternative to the ideal solution and the rankings of different configurations. According to Table 2, the similar upstream wake at close distance (S/D=4) gives the best overall energy performance of the circular oscillator. The order of preference of the circular wake at S/D=4 is $\hat{Z}$ =0.817, which is more than two folds of that in the single configuration. In Table 6, after the circular wake at S/D=4 is the square wake at S/D=4 with the closeness coefficient of 0.391. The isolated circular oscillator is placed third but has a very close energy performance to that under the square wake. Table 2 shows that, dislike the circular wake, the upstream square interfering body does not have a significant energy improvement effects on circular oscillator. This is because of the system's considerably lower efficiency at this configuration.

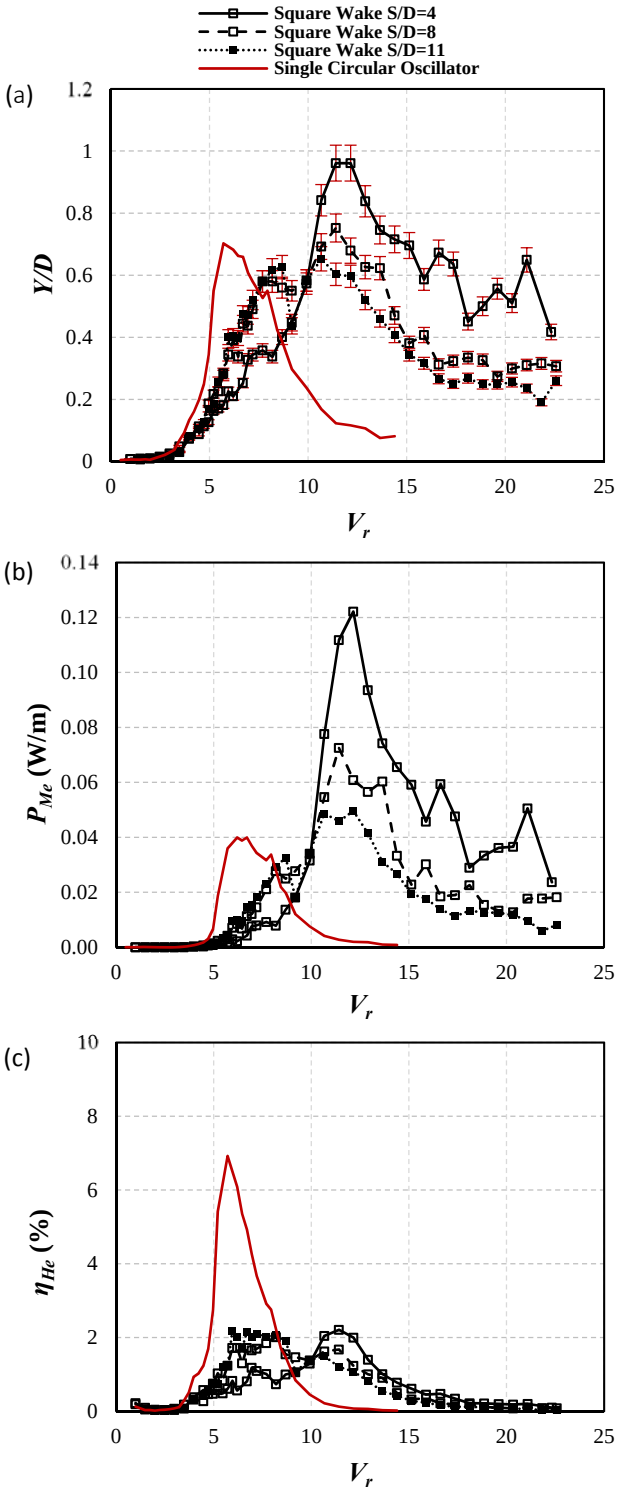

Figure 3. Hydrokinetic energy performance of the circular oscillator at the wake of square cylinder. (a) Transverse response amplitude; (b) Harvested mechanical power; (c)

Hydroelastic efficiency. The propagated error bars are shown on the experimental displacement amplitude curves.

Table 2. The weighted normalized decision matrix, the closeness of each alternative to the ideal solution ($\hat{Z}$) and the rankings of different configurations.

	$\eta_{He\text{-}max}$	$\eta_{He\text{-}mean}$	$P_{Me\text{-}max}$	$P_{Me\text{-}mean}$	$\hat{Z}$	Rank
Isolated Cylinder	0.132	0.149	0.036	0.050	0.389	3
Circular Wake (S/D=4)	0.082	0.152	0.134	0.224	0.817	1
Circular Wake (S/D=8)	0.073	0.125	0.039	0.079	0.293	4
Circular Wake (S/D=11)	0.073	0.116	0.035	0.060	0.240	5
Square Wake (S/D=4)	0.042	0.063	0.109	0.125	0.391	2
Square Wake (S/D=8)	0.039	0.075	0.065	0.085	0.193	6
Square Wake (S/D=11)	0.042	0.077	0.044	0.069	0.106	7

5. CONCLUSIONS

In the present experimental study, the effects of square wake on the flow induced vibration energy harvesting performance of a circular oscillator was investigated. The upstream interfering square cylinder was placed at three different distances from the circular oscillator. The hydroelastic power and efficiency of the mechanical subsystem were calculated and compared against that in single configuration and under circular wake.

The maximum mechanical power of the circular oscillator under square wake was more than 3 times that in single configuration. However, this ratio was reversed in terms of efficiency. Comparing to the circular upstream wake, the square interfering body was less effective in the improvement of the overall energy performance of the circular oscillator.

6. REFERENCE

[1] Khan MJ, Bhuyan G, Iqbal MT, Quaicoe JE. Hydrokinetic energy conversion systems and assessment of horizontal and vertical axis turbines for river and tidal applications: A technology status review. Applied Energy 2009; 86:1823-1835.

[2] Sun W, Zhao D, Tan T, Yan Zh, Guo P, Luo X. Low velocity water flow energy harvesting using vortex induced vibration and galloping. Applied Energy 2019;251:113392.

[3] Liu FR, Zhang WM, Zhao LCH, Zou HX, Tan T, Peng ZhK, Meng G. Performance enhancement of wind energy harvester utilizing wake flow induced by double upstream flat-plates. Applied Energy 2020;257:114034.

[4] Elvin N and Erturk A. Advances in energy harvesting methods. Springer 2013.

[5] Bernitsas MM and Raghavan K. Converter of Current/Tide/Wave Energy. Provisional Patent Application, U.S. Patent and Trademark Office, 2004 Serial No. 60/628,252.

[6] Bernitsas MM, Raghavan K, Ben-Simon Y, Vivace (vortex induced vibrationaquatic clean energy): A new concept in generation of clean and renewableenergy from fluid flow. J. Offshore Mech. Arct. Eng. Trans. ASME 2008;130 041101:1-15.

[7] Abdelkefi A, Hajj MR, Nayfeh AH. Phenomena and modeling of piezoelectric energy harvesting from freely oscillating cylinders. Nonlinear Dynamics, 2012; 70(2), pp.1377-1388.

[8] Soti AK, Thompson MC, Sheridan J, Bhardwaj R. Harnessing electrical power from vortex-induced vibration of a circular cylinder. Journal of Fluids and Structures 2017;70:360-373.

[9] Lee JH, Bernitsas MM. High-damping, high-Reynolds VIV tests for energy harnessing using the VIVACE converter. Ocean Engineering 2011; 38:1697-1712.

[10] Ma C, Sun H, Nowakowski G, Mauer E, Bernitsas MM. Nonlinear piecewise restoring force in hydrokinetic power conversion using flow induced motions of single cylinder. Ocean Engineering 2016; 128, 1-12.

[11] Sun H, Kim ES, Nowakowski G, Mauer E, Bernitsas MM. Effect of mass-ratio, damping, and stiffness on optimal hydrokinetic energy conversion of a single, rough cylinder in flow induced motions. Renewable Energy 2016; 99, 936-959.

[12] Chang CC, Kumar RA, Bernitsas MM.VIV and galloping of single circular cylinder with surface roughness at 3.0x104 $\leqslant$ Re $\leqslant$ 1.2x105. Ocean Eng. 2011;38-16:1713-1732.

[13] Park H, Bernitsas MM, Kumar RA. Enhancement of flow-induced motion of rigid circular cylinder on springs by localized surface roughness at 3.0 x 104 < Re < 1.2x 105. Ocean Eng 2013;72:403-15.

[14] Barrero-Gil A, Alonso G, Sanz-Andres A. Energy harvesting from transverse galloping. Journal of Sound and Vibration 2010;329:2873-2883.

[15] Abdelkefi A, Hajj MR, Nayfeh AH. Piezoelectric energy harvesting from transverse galloping of bluff bodies. Smart Mater. Struct. 2013;22:015014 (11pp).

[16] Ding L, Zhang L, Wu Ch, Maoa X, Jiang D. Flow induced motion and energy harvesting of bluff bodies with different cross sections. Energy Convers. Manage. 2015;91:416-426.

[17] Zhang J, Xu G, Liu F, Lian J, Yan X. Experimental investigation on the flow induced vibration of an

equilateral triangle prism in water. Applied Ocean Research 2016;61:92-100.
[18] Hémon P, Amandolese X, Andrianne T, Energy harvesting from galloping of prisms: A wind tunnel experiment. Journal of Fluids and Structures 2017;70:390-402.
[19] Tamimi V, Naeeni STO, Zeinoddini M, Seif MS, Dolatshahi Pirooz M. Effects of After-body on the FIV of an Isosceles Right-angle Triangular Cylinder in Comparison to Circular, Square, and Diamond Cross-sections. Journal of Ships and Offshore Structures 2018; 14:589-599.
[20] Tamimi V, Armin M, Shahvaghar-Asl S, Naeeni STO, Zeinoddini M. FIV Energy Harvesting from Sharp-edge Oscillators. Proceedings of the ASME 2019 38th International Conference on Ocean, Offshore and Arctic Engineering, OMAE2019, Jun. 9-14, 2019, Glasgow, Scotland.
[21] Assi GRS, Bearman PW, Carmo BS, Meneghini JR, Shervin SJ, Willden RHJ. The role of wake stiffness on the wake-induced vibration of the downstream cylinder of a tandem pair. J Fluid Mech 2013:718.
[22] Kim ES, Bernitsas MM. Performance prediction of horizontal hydrokinetic energy converter using multiple-cylinder synergy in flow induced motion. Applied Energy 2016;170: 92-100.
[23] Sun H, Ma C, Kim ES, Nowakowski G, Mauer E, Bernitsas, MM. Hydrokinetic Energy Conversion by two Rough Tandem-Cylinders in Flow Induced Motions: Effect of Spacing and Stiffness, Renewable Energy 2017;Vol. 107, pp. 61-80.
[24] Tamimi V, Naeeni STO, Zeinoddini M, Bakhtiari A. Effects of upstream sharp edge square and diamond cylinders on the FIV of a circular cylinder. Marine Structures 2018;59:237-250.
[25] Zeinoddini M, Tamimi V, Bakhtiari A. WIV Response of Tapered Circular Cylinders in a Tandem Arrangement: An Experimental Study. Journal of Applied Ocean Research 2014;47:162-17.
[26] Tamimi V, Naeeni STO, Zeinoddini M. Flow induced vibrations of a sharp edge square cylinder in the wake of a circular cylinder. Applied Ocean Research 2017; 66:117-130.
[27] Akbaş H, Bilgen B. An integrated fuzzy QFD and TOPSIS methodology for choosing the ideal gas fuel at WWTPs. Energy 2017;125:484-497.